JYX
JYVÄSKYLÄN YLIOPISTO
UNIVERSITY OF JYVÄSKYLÄ

This is a self-archived version of an original article. This version may differ from the original in pagination and typographic details.

Author(s): Petrache, C. M.; Lv, B. F.; Astier, A.; Dupont, E.; Zheng, K. K.; Greenlees, P. T.; Badran, H.; Calverley, T.; Cox, D. M.; Grahn, T.; Hilton, J.; Julin, R.; Juutinen, S.; Konki, J.; Pakarinen, J.; Papadakis, P.; Partanen, J.; Rahkila, P.; Ruotsalainen, P.; Sandzelius, M.; Saren, J.; Scholey, C.; Sorri, J.; Stolze, S.; Uusitalo, J.; Cederwall, B.; Aktas, Ö.; Ertoprak, A.; Liu, H.; Guo, S.; Liu, M. L.; Wang, J. G.; Zhou, X. H.; Kuti, I.;

Title: Highly deformed bands in Nd nuclei : New results and consistent interpretation within the cranked Nilsson-Strutinsky formalism

Year: 2019

Version: Published version

Copyright: ©2019 American Physical Society

Rights: In Copyright

Rights url: http://rightsstatements.org/page/InC/1.0/?language=en

Please cite the original version:

Petrache, C. M., Lv, B. F., Astier, A., Dupont, E., Zheng, K.K., Greenlees, P. T., Badran, H., Calverley, T., Cox, D. M., Grahn, T., Hilton, J., Julin, R., Juutinen, S., Konki, J., Pakarinen, J., Papadakis, P., Partanen, J., Rahkila, P., Ruotsalainen, P., . . . Andreoiu, C. (2019). Highly deformed bands in Nd nuclei : New results and consistent interpretation within the cranked Nilsson-Strutinsky formalism. Physical Review C, 100(5), Article 054319. https://doi.org/10.1103/PhysRevC.100.054319

Highly deformed bands in Nd nuclei: New results and consistent interpretation within the cranked Nilsson-Strutinsky formalism

C. M. Petrache,[1] B. F. Lv,[1] A. Astier,[1] E. Dupont,[1] K. K. Zheng,[1] P. T. Greenlees,[2] H. Badran,[2] T. Calverley,[2,*] D. M. Cox,[2,†] T. Grahn,[2] J. Hilton,[2,*] R. Julin,[2] S. Juutinen,[2] J. Konki,[2,‡] J. Pakarinen,[2] P. Papadakis,[2,§] J. Partanen,[2] P. Rahkila,[2] P. Ruotsalainen,[2] M. Sandzelius,[2] J. Saren,[2] C. Scholey,[2] J. Sorri,[2,‖] S. Stolze,[2,¶] J. Uusitalo,[2] B. Cederwall,[3] Ö. Aktas,[3] A. Ertoprak,[3] H. Liu,[3] S. Guo,[4] M. L. Liu,[4] J. G. Wang,[4] X. H. Zhou,[4] I. Kuti,[5] J. Timár,[5] A. Tucholski,[6] J. Srebrny,[6] and C. Andreoiu[7]

[1]*Centre de Sciences Nucléaires et Sciences de la Matière, CNRS/IN2P3, Université Paris-Saclay, Bâtiment 104-108, 91405 Orsay, France*
[2]*University of Jyväskylä, Department of Physics, P.O. Box 35, FI-40014 University of Jyväskylä, Finland*
[3]*KTH Department of Physics, S-10691 Stockholm, Sweden*
[4]*Institute of Modern Physics, Chinese Academy of Sciences, Lanzhou 730000, China*
[5]*Institute of Nuclear Research, Hungarian Academy of Sciences, 4001 Debrecen, Hungary*
[6]*University of Warsaw, Heavy Ion Laboratory, Pasteura 5a, 02-093 Warsaw, Poland*
[7]*Department of Chemistry, Simon Fraser University, Burnaby, British Columbia V5A 1S6, Canada*

(Received 13 September 2019; published 15 November 2019)

Three new highly-deformed (HD) bands are identified in ^{136}Nd and the highly deformed band of ^{137}Nd is extended at higher spin by four transitions, revealing a band crossing associated with the occupation of the second $\nu i_{13/2}$ intruder orbital. Extended cranked Nilsson-Strutinsky calculations are performed for all HD bands observed in ^{134}Nd, ^{136}Nd, and ^{137}Nd, achieving for the first time a consistent interpretation of all HD bands in the Nd nuclei. The new interpretation has significant consequences, like the change of parity of the yrast HD bands of ^{134}Nd and ^{136}Nd, and the involvement of two negative-parity neutron intruder orbitals in the configurations of most HD bands. The present experimental results and their theoretical interpretation represent an important step forward in the understanding of the second-minimum excitations in the Nd nuclei.

DOI: 10.1103/PhysRevC.100.054319

I. INTRODUCTION

Superdeformed (SD) and highly deformed (HD) bands in the $A = 130$ mass region were actively studied until 10–15 years ago using high-efficiency Ge-detector arrays for γ-ray detection. The interest in studying these high-spin bands was to understand the superdeformation in the $A = 130$ mass region, where two types of bands have been identified: HD bands in Nd nuclei involving only neutron intruder orbitals $\nu(i_{13/2}, f_{7/2}, h_{9/2})$ from above the $N = 82$ shell closure, and SD bands in Ce nuclei which involve both neutron intruder orbitals and proton extruder orbitals $\pi g_{9/2}$ from below the $Z = 50$ shell closure, leading to larger deformation [1]. However, a very limited number of bands have been linked to low-lying states, mainly in the Nd nuclei, in which the difference in deformation between the HD and the normal-deformed (ND) bands $\beta_2^{HD} - \beta_2^{ND} \approx 0.3$–$0.15$ is lower than in the Ce nuclei $\beta_2^{SD} - \beta_2^{ND} \approx 0.4$–$0.15$, and consequently the barrier between the HD and ND minima is lower than that between the SD and ND minima. This was the experimental reason why the bands in the Ce nuclei have been called superdeformed. In addition, there is also a theoretical reason, related to the presence of holes in the $\pi g_{9/2}$ orbital in the assigned configurations, which is possible at large deformation, like in the SD bands of the $A = 150$ mass region [1]. Fourteen SD bands have been identified in the Ce nuclei from ^{129}Ce to ^{134}Ce [2–10]. None of these bands was linked to low-lying states. This prohibited for a long time definite configuration assignments to the bands. Transition quadrupole moments of several bands have been measured in Ce nuclei [2,11–16]. The most recent experimental results on the SD bands of ^{133}Ce and ^{134}Ce have been published in Refs. [17,18].

In the Nd nuclei, the HD bands involve at least one $\nu i_{13/2}$ intruder orbital, which induces a higher deformation than that of the bands built on neutron orbitals located below the $N = 82$ shell closure. In the light Nd nuclei, which are highly deformed already in the ground state, the occupation of the $\nu i_{13/2}[660]1/2$ intruder orbital was proposed for one band of ^{128}Nd, which is the lightest Nd nucleus known

*Present address: Department of Physics, University of Liverpool, The Oliver Lodge Laboratory, Liverpool L69 7ZE, United Kingdom.
†Present address: Department of Mathematical Physics, Lund Institute of Technology, S-22362 Lund, Sweden.
‡Present address: CERN, CH-1211 Geneva 23, Switzerland.
§Present address: Oliver Lodge Laboratory, University of Liverpool, Liverpool L69 7ZE, United Kingdom.
‖Present address: Sodankylä Geophysical Observatory, University of Oulu, FIN-99600 Sodankylä, Finland.
¶Present address: Physics Division, Argonne National Laboratory, Argonne, Illinois 60439, USA.

 ©2019 American Physical Society

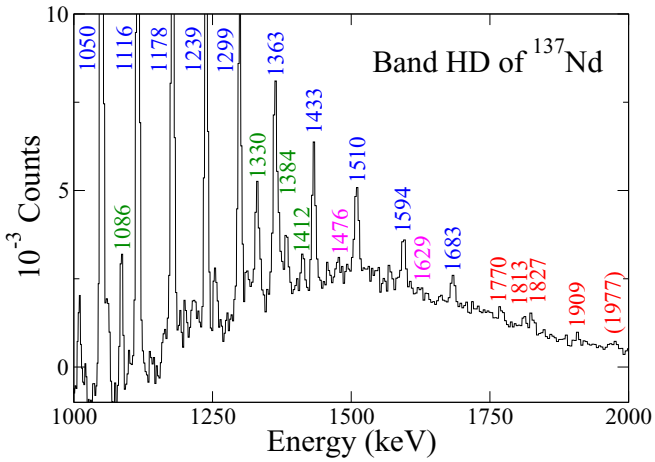

FIG. 1. Spectrum constructed by double gating on all observed transitions of band HD of ^{137}Nd. The new in-band (decay-out) transitions are marked with red (magenta) labels, while the previously known in-band (decay-out) transitions are marked with blue (green) labels, respectively.

spectroscopically [19]. However, an alternative configuration involving the $\nu(s_{1/2}, d_{3/2})[411]1/2$ orbital was also proposed for the same band [20]. The presence of the deformation driving $\nu i_{13/2}$ intruder orbital was also observed at high spin in one band of ^{129}Nd [21]. HD bands developed over extended spin ranges and solid configuration assignments have been identified in Nd nuclei between ^{129}Nd and ^{138}Nd [21–40]. Transition quadrupole moments have been measured for HD bands of ^{133}Nd [27,28,41], ^{134}Nd [12], ^{135}Nd [12,28,42], and ^{137}Nd [27,43].

The present work was triggered by the new results obtained from a high-statistics JUROGAM II experiment [44–49], which allowed us to extend the known HD bands of ^{136}Nd and ^{137}Nd at lower and higher spins and to identify three new HD bands in ^{136}Nd. The HD bands of ^{134}Nd, ^{136}Nd, and ^{137}Nd nuclei are interpreted in the framework of the cranked Nilsson-Strutinsky (CNS) model [50–52]. We included in the present work the analysis of the HD bands of ^{134}Nd because they are all linked to low-lying states and therefore have firmly established spins and parities. Their consistent interpretation can therefore give a solid starting point for the analysis of the HD bands in the neighboring ^{136}Nd, in which four bands are not linked to low-lying states. The HD bands of ^{134}Nd and ^{136}Nd which are linked to low-lying states are well reproduced by the calculations. The energies, spins and parities of the HD bands which are not linked to low-lying states are adjusted to be in agreement with the lowest excited CNS configurations in the high-spin region. The proposed interpretation suggests the involvement of two $\nu[541]1/2$ negative-parity intruder orbitals, leading to positive parity, which is different from the previously reported negative parity of the yrast HD bands of ^{134}Nd and ^{136}Nd, and represents a consistent description of the HD excitations in the second minimum of the Nd nuclei.

II. EXPERIMENT AND RESULTS

High-spin states in ^{136,137}Nd were populated using the ^{100}Mo + ^{40}Ar reaction and a 152-MeV beam of ^{40}Ar, pro-

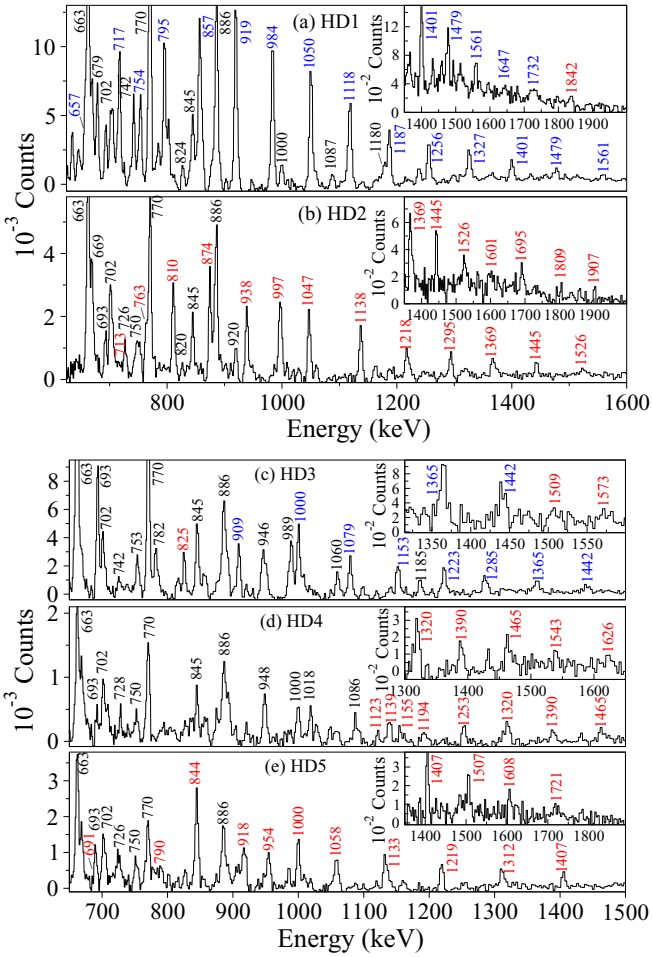

FIG. 2. Spectra constructed by double gating on the observed transitions of the bands HD of ^{136}Nd: (a) and (b) bands with assigned positive parity; (c)–(e) bands with assigned negative parity. The previously known transitions are marked with blue labels, the new transitions marked with red labels, while the coincident ND transitions are marked with black labels.

vided by the K130 Cyclotron at the University of Jyväskylä, Finland. The target consisted of a self-supporting enriched ^{100}Mo foil of 0.5 mg/cm^2 thickness. The ^{135}Nd and ^{136}Nd nuclei were the most strongly populated in the reaction, with cross sections of around 100 mb each. The ^{137}Nd nucleus was populated with a lower cross section of around 2 mb. A number of 5.1×10^{10} threefold and higher prompt γ-ray coincidence events were accumulated using the JUROGAM II array. The events were time-stamped by the Total Data Readout (TDR) data acquisition system [53], and sorted using the GRAIN code [54]. Fully symmetrized, three-dimensional (E_γ-E_γ-E_γ) and four-dimensional (E_γ-E_γ-E_γ-E_γ) matrices were analyzed using the RADWARE [55,56] analysis package.

A double-gated spectrum of band HD of ^{137}Nd is shown in Fig. 1. Double-gated spectra of the three new HD bands HD-2, HD-4, and HD-5 of ^{136}Nd are shown in Fig. 2, together with double-gated spectra of the previously know HD bands (HD1 and HD3 in the present work). The partial level schemes of ^{136}Nd and ^{137}Nd and the table with the experimental information on the new transitions are given Figs. 3 and 4.

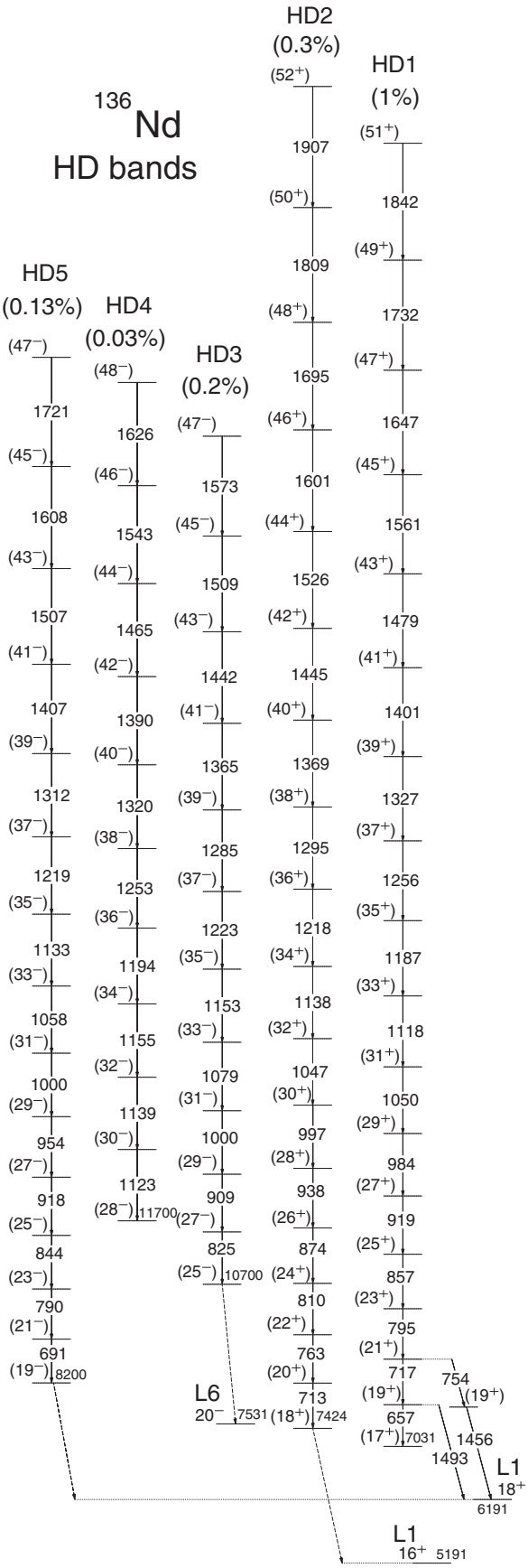

FIG. 3. Partial level scheme of ^{136}Nd showing the HD bands.

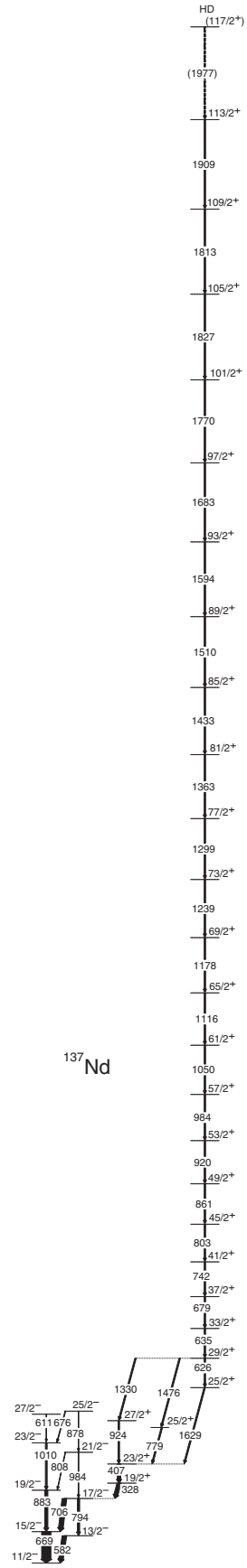

FIG. 4. Partial level scheme of ^{137}Nd showing the HD band.

TABLE I. Experimental information including the γ-ray energies and the spin-parity assignments to the observed states in ^{136}Nd and ^{137}Nd. (The error on the transition energies is 0.2 keV for transitions below 1000 keV, 0.5 keV for transitions above 1000 keV, and 1.0 keV for transitions above 1200 keV.)

γ-ray energy	E_i (keV)	$J_i^\pi \rightarrow J_f^\pi$
Band HD1 of ^{136}Nd		
656.8	7687.8	$(19^+) \rightarrow (17^+)$
717.1	8404.9	$(21^+) \rightarrow (19^+)$
795.2	9200.1	$(23^+) \rightarrow (21^+)$
857.4	10057.5	$(25^+) \rightarrow (23^+)$
919.4	10976.9	$(27^+) \rightarrow (25^+)$
983.6	11960.5	$(29^+) \rightarrow (27^+)$
1050.1	13010.6	$(31^+) \rightarrow (29^+)$
1117.8	14128.4	$(33^+) \rightarrow (31^+)$
1186.5	15314.9	$(35^+) \rightarrow (33^+)$
1256.2	16571.1	$(37^+) \rightarrow (35^+)$
1326.9	17898.0	$(39^+) \rightarrow (37^+)$
1400.5	19298.5	$(41^+) \rightarrow (39^+)$
1479.2	20777.7	$(43^+) \rightarrow (41^+)$
1561.1	22338.8	$(45^+) \rightarrow (43^+)$
1646.8	23985.6	$(47^+) \rightarrow (45^+)$
1732.4	25718.0	$(49^+) \rightarrow (47^+)$
1841.9	27559.9	$(51^+) \rightarrow (49^+)$
Band HD2 of ^{136}Nd		
713.2	8137.2	$(20^+) \rightarrow (18^+)$
762.5	8899.7	$(22^+) \rightarrow (20^+)$
810.1	9709.8	$(24^+) \rightarrow (22^+)$
873.8	10583.6	$(26^+) \rightarrow (24^+)$
938.4	11522.0	$(28^+) \rightarrow (26^+)$
996.5	12518.5	$(30^+) \rightarrow (28^+)$
1047.2	13565.7	$(32^+) \rightarrow (30^+)$
1137.5	14703.2	$(34^+) \rightarrow (32^+)$
1217.8	15921.0	$(36^+) \rightarrow (34^+)$
1294.5	17215.5	$(38^+) \rightarrow (36^+)$
1368.9	18584.4	$(40^+) \rightarrow (38^+)$
1445.2	20029.6	$(42^+) \rightarrow (40^+)$
1525.7	21555.3	$(44^+) \rightarrow (42^+)$
1601.4	23156.7	$(46^+) \rightarrow (44^+)$
1695.4	24852.1	$(48^+) \rightarrow (46^+)$
1808.5	26660.6	$(50^+) \rightarrow (48^+)$
1906.9	28567.5	$(52^+) \rightarrow (50^+)$
Band HD3 of ^{136}Nd		
825.1	11525.1	$(27^-) \rightarrow (25^-)$
908.9	12434.0	$(29^-) \rightarrow (27^-)$
1000.2	13434.2	$(31^-) \rightarrow (29^-)$
1079.4	14513.6	$(33^-) \rightarrow (31^-)$
1152.5	15666.1	$(35^-) \rightarrow (33^-)$
1222.7	16888.8	$(37^-) \rightarrow (35^-)$
1285.2	18174.0	$(39^-) \rightarrow (37^-)$
1365.4	19539.4	$(41^-) \rightarrow (39^-)$
1442.1	20981.5	$(43^-) \rightarrow (41^-)$
1508.5	22490.0	$(45^-) \rightarrow (43^-)$
1573.1	24063.1	$(47^-) \rightarrow (45^-)$
Band HD4 of ^{136}Nd		
1122.7	12822.7	$(30^-) \rightarrow (28^-)$
1139.2	13961.9	$(32^-) \rightarrow (30^-)$
1155.1	15117.0	$(34^-) \rightarrow (32^-)$
1194.0	16311.0	$(36^-) \rightarrow (34^-)$
1252.9	17563.9	$(38^-) \rightarrow (36^-)$
1320.4	18884.3	$(40^-) \rightarrow (38^-)$
1390.3	20274.6	$(42^-) \rightarrow (40^-)$
1464.8	21739.4	$(44^-) \rightarrow (42^-)$
1542.7	23282.1	$(46^-) \rightarrow (44^-)$
1626.4	24908.5	$(48^-) \rightarrow (46^-)$
Band HD5 of ^{136}Nd		
690.5	8890.5	$(21^-) \rightarrow (19^-)$
790.4	9680.9	$(23^-) \rightarrow (21^-)$
844.2	10525.1	$(25^-) \rightarrow (23^-)$
917.5	11442.6	$(27^-) \rightarrow (25^-)$
953.9	12396.5	$(29^-) \rightarrow (27^-)$
1000.3	13396.8	$(31^-) \rightarrow (29^-)$
1058.1	14454.9	$(33^-) \rightarrow (31^-)$
1132.5	15587.4	$(35^-) \rightarrow (33^-)$
1218.5	16805.9	$(37^-) \rightarrow (35^-)$
1312.0	18117.9	$(39^-) \rightarrow (37^-)$
1407.3	19525.2	$(41^-) \rightarrow (39^-)$
1507.2	21032.4	$(43^-) \rightarrow (41^-)$
1608.4	22640.8	$(45^-) \rightarrow (43^-)$
1720.5	24361.3	$(47^-) \rightarrow (45^-)$
Band HD of ^{137}Nd		
625.8	4883.1	$29/2^+ \rightarrow 25/2^+$
634.9	5518.0	$33/2^+ \rightarrow 29/2^+$
678.7	6196.7	$37/2^+ \rightarrow 33/2^+$
741.9	6938.6	$41/2^+ \rightarrow 37/2^+$
802.6	7741.2	$45/2^+ \rightarrow 41/2^+$
861.5	8602.7	$49/2^+ \rightarrow 45/2^+$
920.5	9523.2	$53/2^+ \rightarrow 49/2^+$
984.1	10507.3	$57/2^+ \rightarrow 53/2^+$
1050.1	11557.4	$61/2^+ \rightarrow 57/2^+$
1115.5	12672.9	$65/2^+ \rightarrow 61/2^+$
1178.0	13850.9	$69/2^+ \rightarrow 65/2^+$
1238.7	15089.6	$73/2^+ \rightarrow 69/2^+$
1298.9	16388.5	$77/2^+ \rightarrow 73/2^+$
1362.7	17751.2	$81/2^+ \rightarrow 77/2^+$
1432.6	19183.8	$85/2^+ \rightarrow 81/2^+$
1509.8	20693.6	$89/2^+ \rightarrow 85/2^+$
1594.1	22287.7	$93/2^+ \rightarrow 89/2^+$
1683.3	23971.0	$97/2^+ \rightarrow 93/2^+$
1770.0	25741.0	$101/2^+ \rightarrow 97/2^+$
1827.0	27568.0	$105/2^+ \rightarrow 101/2^+$
1812.8	29380.8	$109/2^+ \rightarrow 105/2^+$
1909	31289.8	$113/2^+ \rightarrow 109/2^+$
(1977)	33266.8	$(117/2^+) \rightarrow 113/2^+$

The experimental information on the observed states in ^{136}Nd and ^{137}Nd are given in Table I.

We observed five new levels (the highest one being tentative) which decay via the 1770, 1827, 1813, and 1909 keV (and a tentative 1977-keV transition) on top of the HD band of ^{137}Nd. A crossing is observed at spin around $105/2\,\hbar$, which is associated with a gain in alignment of a few units of spin. A new transition of 625.8 keV has been identified at

the bottom of the HD band, which now is based on the $25/2^+$ state at 4257.3 keV. Two new decay-out transitions have also been identified (see Fig. 4): 1475.6 and 1629.0 keV from the $29/2^+$ and $25/2^+$ states of the HD band, to the $25/2^+$ state at 3411 keV and the $23/2^+$ state at 2631 keV, respectively [38].

The highest transition of band HD yrast of ^{136}Nd (HD1 in the present work) of 1815 keV reported previously [37] is not observed; we observed instead one new transition of 1842 keV on top of the band. The excited HD band reported previously [35] (HD3 in the present work), has been extended to lower spins by one transition of 825 keV. The highest 1525-keV transition of band HD3 reported previously is not observed in the present data. We observe two new transitions of 1509 and 1573 keV on top of band HD3. Three new HD bands (HD2, HD4 and HD5) are identified in the present work. The intensities of the bands normalized to the relative intensity of band HD1, which is around 1%, are 0.3% for HD2, 0.2% for HD3, 0.03% for HD4, and 0.13% for HD5.

III. BAND STRUCTURE ANALYSIS

In the CNS formalism, the nucleus rotates about one of its principal axes and pairing is neglected. The deformation is optimized for each configuration. The configurations are labeled by the number of particles in low-j and high-j orbitals, in the different $\mathcal{N}$ shells. They can be defined relative to a ^{132}Sn core as

$$\pi(dg)^{p_1}(h_{11/2})^{p_2}\nu[(dg)(sd)]^{-n_1}(h_{11/2})^{-n_2}(hf)^{n_3}(i_{13/2})^{n_4},$$

for which the short-hand notation $[p_1p_2, n_1n_2(n_3n_4)]$ is used. The pseudospin partners $d_{5/2}g_{7/2}$ (dg) and $s_{1/2}d_{3/2}$ (sd) are not distinguished in the CNS formalism. Note that all particles are listed and not just those considered as active (unpaired). Note also that the labels do not refer to the pure j shells, but rather to the dominating amplitudes in the Nilsson orbitals. For an odd number of particles in a group, the signature is specified as a subscript $+$ $(\alpha = +1/2)$ or $-$ $(\alpha = -1/2)$. We will use the so-called Lund convention for the triaxiality parameter γ in relation to the main rotation axis, where for the positive γ shape, $0 < \gamma < 60^\circ$, the rotation (x) axis is the shortest principal axis, while for the negative γ shape, $-60^\circ < \gamma < 0$, it is the intermediate principal axis. In the present calculations the $A = 130$ parameters are used. They are identical with the $A = 110$ parameters [57] in the valence space, $N = 4, 5$, but with μ increased from 0.34 to 0.40 for neutrons in the $N = 6$ shell [58] in order to get the $i_{13/2}$ neutron subshell at a lower energy and furthermore with μ increased from 0.52 to 0.60 for the higher proton shells, $N \geqslant 6$.

In the present work we will also use the short notation 5^x6^y, which includes only the intruder orbitals $[(\nu h_{9/2}/f_{7/2})^x(\nu i_{13/2})^y]$. In order to facilitate the understanding of the configuration assignments, we include a neutron single-particle Routhian diagram calculated for ^{136}Nd at a typical deformation of $\epsilon_2 = 0.30$, $\epsilon_4 = 0.016$, and $\gamma = 0^\circ$ in Fig. 5. One can compare it with the similar neutron single-particle Routhian diagram shown in Fig. 3(c) of [30], which was calculated for ^{134}Nd at the same deformation using a Woods-Saxon potential, and observe their resemblance. This

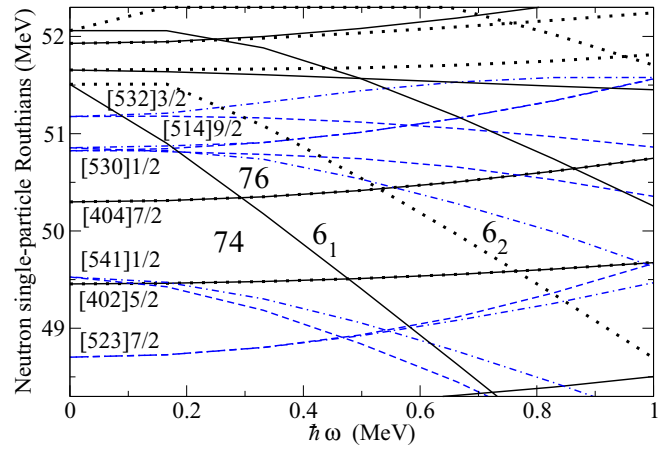

FIG. 5. Single-particle neutron Routhians for ^{136}Nd calculated at $\epsilon_2 = 0.30$, $\epsilon_4 = 0.016$, and $\gamma = 0^\circ$. Signature and parity of the states are as follows: black solid $= (+, +1/2)$, black dashed $= (+, -l/2)$, blue dashed $= (-, +1/2)$, blue dashed-dotted $= (-, -l/2)$. The relevant orbitals for the present discussion are indicated as follows: the neutron orbitals are labeled with the asymptotic Nilsson quantum numbers, while the signature partners of the $i_{13/2}$ intruder orbital are labeled with 6_1 and 6_2.

gives us additional confidence in the configuration assignments based on the present CNS calculations.

The present study is mainly devoted to the newly observed HD bands of ^{136}Nd. However, in order to qualify the proposed theoretical interpretation based on CNS calculations, we first calculated the neighboring ^{134}Nd nucleus, in which all HD bands have been linked to low-lying states and therefore have firm energies and spins. We then calculated the HD configurations of ^{136}Nd and tried to obtain a coherent interpretation of the HD bands in both ^{134}Nd and ^{136}Nd. Finally we calculated the HD band of ^{137}Nd, investigating the origin of the observed crossing at high spins. In the following we discuss the obtained results and the configuration assignments, which led us to achieve a new view of the excitations in the second minimum of Nd nuclei.

The calculated results for all three nuclei ^{134}Nd, ^{136}Nd, and ^{137}ND are shown in Fig. 6, in which the experimental bands are shown in panels (a), (d), and (g), the calculated bands are shown in panels (b), (e), and (h), and the differences between CNS calculations and the experimental bands are shown in panels (c), (f), and (i).

IV. DISCUSSION

The observed bands of ^{134}Nd and their evolution at high spin represent a unique set of HD bands which are all linked to low-lying states, and therefore have experimentally determined excitation energies and spins. A comprehensive discussion of all bands using the cranked Strutinsky approach based on the Woods-Saxon potential including pairing interaction has been reported in Refs. [29,30]. The present CNS calculations show that in the spin range $I = 25\hbar$–$40\hbar$, in which the HD bands involve only one $\nu i_{13/2}$ intruder orbital, the calculated deformations are nearly prolate and rather stable,

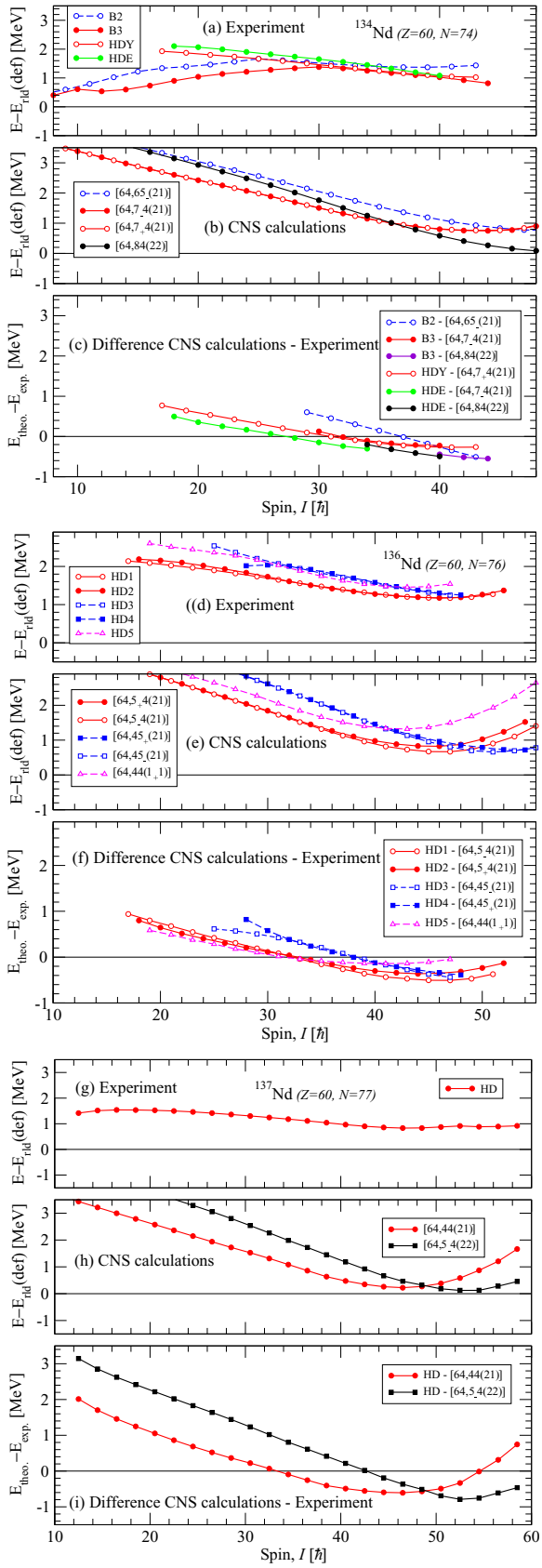

FIG. 6. Comparison between the experimental and calculated CNS configurations of the HD bands of ^{134}Nd, ^{136}Nd, and ^{137}Nd.

with values decreasing slightly with increasing spins, from $(\varepsilon_2, \gamma) \approx (0.32, 4^\circ)$ and $(\varepsilon_2, \gamma) \approx (0.28, 8^\circ)$. The deformation of the bands involving two $\nu i_{13/2}$ intruder orbitals, is, as expected, larger at spin $I \approx 40\hbar$, i.e., $(\varepsilon_2, \gamma) \approx (0.34, 4^\circ)$.

The high-spin part of the negative-parity band B2 of ^{134}Nd (band 2 in Ref. [30]) above spin 27^- has a $5^2 6^1$ configuration ([64, 65_(21)] in CNS notation), involving therefore three neutron intruder orbitals. The positive-parity band B3 (band 3 in Ref. [30]), which involves a pair of $\pi h_{11/2}$ protons above 10^+, exhibits a smooth alignment of the $h_{11/2}$ and $h_{9/2}$ neutrons in the spin range $I = 10\hbar$–$30\hbar$, increasing progressively the deformation towards a HD shape, at which the successive occupation of the 6^1 and 6^2 orbitals through crossings with the $\nu[402]5/2^+$ orbitals was experimentally observed. In CNS notation, the two successive HD configurations $5^2 6^1$ and $5^2 6^2$ of band B3 are [64, 7_4(21)] and [64,84(22)], respectively.

Differently from the bands B2 and B3 which evolve from low-spin ND to high-spin HD configurations, the band HDY ("HD yrast" in Ref. [30]) is observed only at high spins, where the 6^1 intruder orbital is occupied. A configuration involving the two opposite-parity orbitals $\nu h_{9/2}/f_{7/2}$ and $\nu i_{13/2}$ ([64,64(11)] in CNS notation) was assigned in Ref. [30], suggesting therefore a negative parity for band HDY. However, in the CNS calculation this configuration is very non-yrast and therefore can be safely discarded. The most natural configuration is [64, 7$_+$4(21)], the signature partner of the [64, 7_4(21)] configuration assigned to band B3 in the corresponding spin region, which nicely reproduces the near degeneracy of bands B3 and HDY, induced by the occupation of the two degenerate signatures of the $\nu d_{5/2}[402]$ orbital (see Fig. 3 and Fig. 3(c) of Ref. [30]).

Band HDE ("HD excited" in Ref. [30]) decays via high-energy transitions to positive-parity bands with even spins. Most probably it has even spins, as assigned in Ref. [30], since a spin lower by $1\hbar$ would make it unrealistically non-yrast. At low spins it is parallel and slightly more excited than band HDY, suggesting the occupation of only one $\nu i_{13/2}$ intruder, and therefore a $5^2 6^1$ configuration ([64, 7_4, (21)] in CNS notation), which is identical to that assigned to band B3. At this point we should remember that in the CNS formalism the pseudospin partners $d_{5/2}$ and $g_{7/2}$ are not distinguished. We can therefore propose the occupation of the $\nu g_{7/2}[404]$ orbital in the configuration of band HDE. The energy of the $\nu g_{7/2}[404]$ orbital is 0.5–1 MeV higher than that of $\nu d_{5/2}[402]$ (see, e.g., Fig. 3 and Fig. 3(c) of Ref. [30]), which well accounts for the higher excitation of band HDE relative to the nearly degenerate bands B3 and HDY involving the $\nu d_{5/2}[402]$ orbital.

We can therefore conclude that the CNS and the Total Routhian surface (TRS) calculations for ^{134}Nd are in agreement, except for the band HDY which is now interpreted as signature partner of band B3.

The configurations assigned to the HD bands of ^{136}Nd involve only one $\nu i_{13/2}$ intruder over the entire observed spin range, since no crossings are observed at high spins, as in the case of ^{134}Nd. The missing crossings are nicely explained by the calculated deformations, which, differently from those

TABLE II. Experimental information and configuration assignment for the HD bands of Nd nuclei. The intruder orbitals $\nu i_{13/2}$ and $\nu(h_{9/2}, f_{7/2})$ are labeled as 6^1 or 5^1, respectively.

HD band	E_x (MeV)	Spin range	$J^{(2)}$ ($\hbar^2$/MeV)	Q_t (eb) [Ref.]	Configuration [Ref.]
^{128}Nd					
Band 2	2.227	$7^- - 21^-$	$25 - 60$		$5^1 6^1$ [19] or ν[411]1/2[523]7/2 [20]
^{129}Nd					
Band 4 ($\alpha = 1/2$)	≈ 5.5	$\approx 20.5^+ - 34.5^+$			6^1 [21]
^{130}Nd					
Band 5	$\approx$3.0	$\approx 11^- - 29^-$	$\approx$60		$5^1 6^1$ [22]
^{131}Nd					
Band 5	4.163	$16.5^+ - 20.5^+$	$\approx$60		6^1 [23]
^{132}Nd					
HD-1	5.673	$17^- - 43^-$	$\approx$60		6^1[523]7/2$^-$ [24]
HD-2	6.164	$18^+ - 42^+$	$\approx$60		6^1[411]1/2$^+$ [24]
HD-3a	6.224	$(17, 18)^+ - (43, 44)^+$	$\approx$60		6^1[402]5/2$^+$ [24]
HD-3b	6.590	$(18, 19)^+ - (42, 43)^+$	$\approx$60		6^1[402]5/2$^+$ [24]
^{133}Nd					
Band 5	2.028	$8.5^+ - 44.5^+$	$\approx$60	$\approx$6 [27,28,41]	6^1 [25]
^{134}Nd					
HD-yrast	6.303	$17^- - 43^-$	$\approx$60	$\approx$6.8 [12]	$5^1 6^1_1$ [29] $\rightarrow 5^2 6^1$
HD-excited	6.834	$18^+ - 40^+$	$\approx$55	$\approx$6.4 [12]	6^1_2[402]5/2 [29] $\rightarrow 5^2 6^1$
Band 2-high	10.351	$27^- - 43^-$	$\approx$50		6^1_1[523]7/2 [30] $\rightarrow 5^2 6^1$
Band 3-high-1	12.951	$32^+ - 40^+$	$\approx$60	$\approx$6.1 [12]	6^1_1[402]5/2 [30]$\rightarrow 5^2 6^2$
Band 3-high-2	19.535	$42^+ - 44^+$			6^2 [30] $\rightarrow 5^2 6^2$
^{135}Nd					
SD	3.323	$12.5^+ - 38.5^+$	$\approx$60	$\approx$7.3[12,42], $\approx$5.7 [28]	6^1 [33]
^{136}Nd					
HD-1	7.031	$17^+ - 51^+$	$\approx$60		$5^2 6^1$ [present work]
HD-2	7.420	$18^+ - 52^+$	$\approx$60		$5^2 6^1$ [present work]
HD-3	≈ 9.3	$25^- - 47^-$	$\approx$60		$5^2 6^1$ [present work]
HD-4	≈ 10.3	$28^- - 48^-$	$\approx$60		$5^2 6^1$ [present work]
HD-5	≈ 7.5	$19^- - 47^-$	$\approx$40		$5^1 6^1$ [present work]
^{137}Nd					
Band 9-low	4.885	$14.5^+ - 28.5^+$	$\approx$60	$(5.2 - 2.7)$ [43], 4.0 [27]	6^1 [38]
Band 9-medium	4.885	$28.5^+ - 52.5^+$	$\approx$60	$(5.2 - 2.7)$ [43], 4.0 [27]	$5^2 6^1$ [38,43]
Band 9-high	27.575	$52.5^+ - 58.5^+$	$\approx$50		$5^2 6^2$ [present work]
^{138}Nd					
HD	≈ 10.5	$\approx 26^+ - 48^+$	$\approx$60		$5^2 6^2$ [40]

of ^{134}Nd, decrease with increasing spins from $\varepsilon_2 \approx 0.30$ to $\varepsilon_2 \approx 0.25$, associated with a significant increase of triaxiality from $\gamma \approx 5^\circ$ to $\gamma \approx 25^\circ$ in the spin range $I = 15\hbar$–$50\hbar$. This calculated softness of ^{136}Nd in the γ direction, which is also present in the HD band of the odd-even neighbor ^{137}Nd (see, e.g., Ref. [43] and Fig. 5 of Ref. [47]), is the reason why no sharp crossings are observed up to very high spins, since the decreasing quadrupole deformation pushes the crossings of the $\nu i_{13/2}$ intruder orbitals with the $\nu d_{5/2}$[402] and $\nu g_{7/2}$[404] ones at higher rotational frequencies (see Fig. 3).

Band HD1 of ^{136}Nd has been previously linked to low-lying states [36], and therefore has firmly established excitation energies and spins. The negative parity was assigned based on TRS calculations which suggest the $5^1 6^1$ configuration. The present experimental data and CNS calculations suggest instead a $5^2 6^1$ ([64, 5_4(21)] in CNS notation) positive-parity configuration, which has a minimum at $I \approx 47\hbar$ in the $(E - E_{rld})$ versus I plot, clearly higher than those of the $5^1 6^1$ configurations at $I \approx 40\hbar$ [see Fig. 4(e)]. As the [64, 5_4(21)] configuration is nearly degenerate with its signature partner [64, 5$_+$4(21)], we adjusted the energies and spins of the newly observed band HD2, second most intense populated in the reaction, to get it nearly degenerate with band HD1. In these conditions, band HD2 has a pattern strikingly similar to that of band HD1, inducing us to assign the $5^2 6^1$ ([64, 5$_{-,+}$4(21)] in CNS notation) configurations to bands HD1, HD2.

The previously observed excited HD band (HD3 in the present work) is confirmed, and a new band, HD4, is observed. HD4 can become nearly degenerate with HD3 if one adjusts adequately their energies and spins. The resulting nearly degenerate pair (HD3, HD4) has a $E - E_{rld}$ minimum at spins definitely larger than those of the (HD1, HD2) pair, suggesting

thus configurations with a larger number of occupied high-j orbitals. Scanning among the possible candidates, it became clear than the configurations with one additional neutron-hole in $\nu h_{11/2}$ lead to minima in the $E - E_{rld}$ plot at higher spin, inducing us to assign the $5^2 6^1$ ([64, $45_{-,+}$(21)] in CNS notation) configuration to bands HD3, HD4.

Band HD5 has a different pattern than the other HD bands of ^{136}Nd, presenting an $E - E_{rld}$ minimum at lower spin of around $41\hbar$. This suggests a configuration with a lower number of intruder orbitals, and the lowest suitable configuration appears to be $5^1 6^1$ ([64, $44(1_+1)$] in CNS notation).

The HD band of ^{137}Nd has been extended to higher spins by five transitions, revealing the presence of a crossing at spin around $105/2\,\hbar$. This is important, because it gives the opportunity to evaluate the adequacy of the adopted $A = 130$ parameters for the Nilsson potential. As one can see in Fig. 4(h), a crossing at spins around $96/2\,\hbar$ between the $5^2 6^1$ and $5^2 6^2$ configurations is calculated, which can be associated with the observed crossing at around $105/2\,\hbar$. The difference of $\approx 4\hbar$ between the observed and calculated crossing spins is to be attributed to the adopted model parameters. In any case, one can consider that a difference of the order of 10% between the calculated and observed crossing spins is a good agreement.

A global view of the experimental properties and the configuration assignment for the HD bands in Nd nuclei is given in Table II.

V. SUMMARY

Summarizing, we experimentally observed three new HD bands in ^{136}Nd and extended the HD bands of ^{136}Nd and ^{137}Nd to lower and higher spins by several transitions. The new results are interpreted by extended CNS calculations performed not only for the HD band of ^{136}Nd but also for those of ^{134}Nd and ^{137}Nd, which are linked to low-lying states and give a solid base to the interpretation of the HD bands of ^{136}Nd. A consistent description of the HD bands is achieved, which gives a new view of the single-particle excitations in the second minimum of the Nd nuclei. The adequacy of the CNS model to investigate the high-spin excitations in nuclei is demonstrated, this time contributing to solve ambiguities of the previous interpretations. The present results point to the necessity to further pursue the investigation of HD bands both experimentally, to firmly establish their energies, spins, parities, and quadrupole moments, and theoretically, to confirm, through different self-consistent approaches, the newly proposed interpretation.

ACKNOWLEDGMENTS

We would like to thank Prof. Ingemar Ragnarsson for the valuable discussion and enlightening comments on the manuscript. This work has been supported by the Academy of Finland under the Finnish Centre of Excellence Programme (2012–2017), by the EU 7th Framework Programme Project No. 262010 (ENSAR), by the US DOE under Contracts No. DEFG02-95ER-40934, by the National Research, Development and Innovation Fund of Hungary (Project No. K128947), by the European Regional Development Fund (Contract No. GINOP-2.3.3-15-2016-00034), by the National Research, Development and Innovation Office NKFIH, Contract No. PD124717, by the Polish National Science Centre Grant No. 2013/10/M/ST2/00427, by the Swedish Research Council under Grant No. 621-2014-5558, by the Chinese Major State 973 Program No. 2013CB834400, by the National Natural Science Foundation of China (Grants No. 11335002, No. 11375015, No. 11461141002, and No. 11621131001), and by the Natural Sciences and Engineering Research Council of Canada (NSERC). The use of germanium detectors from the GAMMAPOOL is acknowledged.

[1] A. V. Afanasjev and I. Ragnarsson, Nucl. Phys. A **608**, 176 (1996).
[2] A. Galindo-Uribarri *et al.*, Phys. Rev. C **54**, R454 (1996).
[3] A. T. Semple *et al.*, J. Phys. G **24**, 1125 (1998).
[4] J. N. Wilson *et al.*, Phys. Rev. C **55**, 519 (1997).
[5] Y.-X. Luo, J.-Q. Zhong, D. J. G. Love, A. Kirwan, P. J. Bishop, M. J. Godfrey, I. Jenkins, P. J. Nolan, S. M. Mullins, and R. Wadsworth, Z. Phys. A **329**, 125 (1988).
[6] A. T. Semple *et al.*, Phys. Rev. C **54**, 425 (1996).
[7] E. S. Paul *et al.*, Phys. Rev. C **71**, 054309 (2005).
[8] D. Santos *et al.*, Phys. Rev. Lett. **74**, 1708 (1995).
[9] K. Hauschild *et al.*, Phys. Lett. B **353**, 438 (1995).
[10] N. J. O'Brien, A. Galindo-Uribarri, V. P. Janzen, D. T. Joss, P. J. Nolan, C. M. Parry, E. S. Paul, D. C. Radford, R. Wadsworth, and D. Ward, Phys. Rev. C **59**, 1334 (1999).
[11] R. M. Clark *et al.*, Phys. Rev. Lett. **76**, 3510 (1996).
[12] C. M. Petrache *et al.*, Phys. Rev. C **57**, R10 (1998).
[13] Y. He *et al.*, J. Phys. G **16**, 657 (1990).
[14] S. M. Mullins *et al.*, Phys. Lett. B **312**, 272 (1993).
[15] A. J. Kirwan, G. C. Ball, P. J. Bishop, M. J. Godfrey, P. J. Nolan, D. J. Thornley, D. J. G. Love, and A. H. Nelson, Phys. Rev. Lett. **58**, 467 (1987).
[16] K. Hauschild *et al.*, Phys. Rev. C **52**, R2281 (1995).
[17] A. D. Ayangeakaa *et al.*, Phys. Rev. C **93**, 054317 (2016).
[18] C. M. Petrache *et al.*, Phys. Rev. C **93**, 064305 (2016).
[19] C. M. Petrache *et al.*, Eur. Phys. J. A **12**, 139 (2001).
[20] O. Zeidan *et al.*, Phys. Rev. C **66**, 044311 (2002).
[21] O. Zeidan *et al.*, Phys. Rev. C **65**, 024303 (2002).
[22] D. J. Hartley *et al.*, Phys. Rev. C **63**, 024316 (2001).
[23] D. J. Hartley *et al.*, Phys. Rev. C **60**, 041301(R) (1999).
[24] C. M. Petrache *et al.*, Phys. Lett. B **415**, 223 (1997).
[25] D. Bazzacco *et al.*, Phys. Rev. C **58**, 2002 (1998).
[26] R. Wadsworth *et al.*, J. Phys. G **13**, L207 (1987).
[27] S. M. Mullins, I. Jenkins, Y.-J. He, A. J. Kirwan, P. J. Nolan, J. R. Hughes, R. Wadsworth, and R. A. Wyss, Phys. Rev. C **45**, 2683 (1992).
[28] F. G. Kondev *et al.*, Phys. Rev. C **60**, 011303(R) (1999).
[29] C. M. Petrache *et al.*, Phys. Lett. B **335**, 307 (1994).

[30] C. M. Petrache *et al.*, Phys. Lett. B **387**, 31 (1996).
[31] C. M. Petrache, Z. Phys. A **358**, 225 (1997).
[32] E. M. Beck *et al.*, Phys. Lett. B **195**, 531 (1987).
[33] E. M. Beck, F. S. Stephens, J. C. Bacelar, M. A. Deleplanque, R. M. Diamond, J. E. Draper, C. Duyar, and R. J. McDonald, Phys. Rev. Lett. **58**, 2182 (1987).
[34] M. A. Deleplanque *et al.*, Phys. Rev. C **52**, R2302 (1995).
[35] C. M. Petrache *et al.*, Phys. Lett. B **373**, 275 (1996).
[36] S. Perriès *et al.*, Phys. Rev. C **60**, 064313 (1999).
[37] R. M. Clark *et al.*, Phys. Lett. B **343**, 59 (1995).
[38] C. M. Petrache *et al.*, Nucl. Phys. A **617**, 228 (1997).
[39] S. Lunardi, R. Venturelli, D. Bazzacco, C. M. Petrache, C. Rossi-Alvarez, G. de Angelis, G. Vedovato, D. Bucurescu, and C. Ur, Phys. Rev. C **52**, R6 (1995).
[40] S. Lunardi *et al.*, Phys. Rev. C **69**, 054302 (2004).
[41] S. A. Forbes *et al.*, Z. Phys. A **352**, 15 (1995).
[42] P. Willsau *et al.*, Phys. Rev. C **48**, R494 (1993).
[43] C. M. Petrache *et al.*, Phys. Lett. B **383**, 145 (1996).
[44] C. M. Petrache *et al.*, Phys. Rev. C **97**, 041304(R) (2018).
[45] Q. B. Chen, B. F. Lv, C. M. Petrache, and J. Meng, Phys. Lett. B **782**, 744 (2018).
[46] B. F. Lv *et al.*, Phys. Rev. C **98**, 044304 (2018).
[47] C. M. Petrache *et al.*, Phys. Rev. C **99**, 041301(R) (2019).
[48] B. F. Lv *et al.*, Phys. Rev. C **100**, 024314 (2019).
[49] C. M. Petrache *et al.* (unpublished).
[50] A. Afanasjev, D. Fossan, G. Lane, and I. Ragnarsson, Phys. Rep. **322**, 1 (1999).
[51] T. Bengtsson and I. Ragnarsson, Nucl. Phys. A **436**, 14 (1985).
[52] B. G. Carlsson and I. Ragnarsson, Phys. Rev. C **74**, 011302 (2006).
[53] I. H. Lazarus *et al.*, IEEE Trans. Nucl. Sci. **48**, 567 (2001).
[54] P. Rahkila, Nucl. Instrum. Methods Phys. Res., Sect. A **595**, 637 (2008).
[55] D. Radford, Nucl. Instrum. Methods Phys. Res., Sect. A **361**, 297 (1995).
[56] D. Radford, Nucl. Instrum. Methods Phys. Res., Sect. A **361**, 306 (1995).
[57] J.-y. Zhang, N. Xu, D. B. Fossan, Y. Liang, R. Ma, and E. S. Paul, Phys. Rev. C **39**, 714 (1989).
[58] R. Wadsworth *et al.*, Phys. Rev. C **62**, 034315 (2000).